

Approximate Performance Assessment of Composite Connector at High Velocity Vehicle Impact

Suman Roy*

*(Department of Civil and Environmental Engineering, Utah State University, Logan, USA

Email: sumanroy74@gmail.com)

ORCID : <https://orcid.org/0000-0003-3446-4666> (Suman Roy)

Abstract:

The increased occurrence of dynamic loading on traditional reinforced concrete (RC) bridge piers caused by natural and man-made impact have been common incidents. Data captured from different articles corroborates that while seismic and blast have received significant attention in the literature, the frequency of crash occurrence due to vehicular impact is considerably higher and warrants additional scrutiny. In addition to the frequency of occurrence of vehicular impact, new construction methods including materials, such as grouted coupler with reinforcing steel bar connections utilized in accelerated bridge construction (ABC), also require an in-depth investigation on the post-crash performance under high velocity vehicle impact. This present study scrutinizes the static and dynamic performances of grouted couplers embedded in a RC ABC pier foundation. Analytical results by using dynamic amplification factor (DAF) are validated with the developed numerical models using finite element (FE) method for single coupler subject to the combination of the apportioned axial and impact loads. Manufacturer provided material's data are used for building up FE model. Static and dynamic impact simulations are carried out to scrutinize the material properties for post impact performance. The DAF is then used to evaluate probability of failure, and the corresponding reliability index of the connector and reinforcing steel bar at ABC bridge pier-foundation connection. Material properties are further scrutinized through integrity analyses and direct reliability method from the extracted results of stress and strain. This study presents valuable information and usefulness to aid in the selection of the appropriate coupler composite embedded at ABC.

Keywords —Accelerated Bridge Construction (ABC), Vehicle Impact Analysis, Numerical Analysis, and Reliability Assessment.

I. INTRODUCTION

Crashworthiness of bridge piers due to exposed face often experience high strain rate dynamic impact. This causes extreme loading events such as natural loads like seismic and wind blast, and man-made as blasting and high velocity vehicular collisions. These events may cause structural health deterioration of the traditional reinforced concrete (RC) bridge pier ranging from trivial damage to severe and catastrophic failure. Health evaluation of the structural elements to predict post seismic performance have received significant attention in high earthquake prone states of the western part of the United States (USA) [1]. Extensive research efforts have been executed to improve the capacity of the piers to resist damage during after seismic events. In addition, the complex mechanisms involved in dynamic impact load events, such as vehicular collisions, on the other hand, have received less attention despite high frequency of occurrences and warrant rigorous investigation [2, 3]. High velocity vehicle impact loading encountered by reinforced concrete (RC) bridge piers triggers serviceability of bridge pier. However, the majority of the existing literature focuses on identifying severity of damage and increasing survivability [4, 5]. However, inadequate attention has been given to estimate the residual capacity of bridge piers encountering vehicle impact that results in low and medium to cosmetic damage. Additionally, the performance of RC bridge piers under vehicle impact has yet to be fully investigated for recent developments associating different materials, geometries, and various impact conditions.

Recently, in addition, non-traditional RC bridge piers are used in the accelerated bridge construction (ABC) method has been increasingly utilized as it decreases construction time, provides improved safety, durability, and reliability compared to the traditional cast-in-place RC bridge piers [6, 7]. However, the short duration high velocity impact and its post-performance of the ABC bridge pier is still relatively unknown. In ABC, connectors such as splice-sleeves and grouted couplers are commonly used to connect different bridge components such as foundation caps to piers. The introduction of these new materials and connection types change the dynamic response of bridge structures due to the fact that they typically have higher stiffness than reinforcing steel. Because of producing discontinuities of the reinforcing steel, the alteration of the energy has been occurred via dissipation path [8]. This study evaluates the performance of a singular grouted coupler section used in foundation-pier connections for ABC against short duration high velocity vehicle impact to predict the coupler behavior, material property, contribution to the response, and post impact shear performance [9]. A prototypical splice-sleeve and grouted coupler connection is analyzed to determine its impact performance for static and dynamic responses to determine its dynamic amplification factor (DAF), followed by determining performance reliability of the coupler via integrity analyses [10] from numerically analyzed results,

1. Introduction

whereas simplified approximation method [11] and compared with the results determined from direct reliability method. Simplified approximation method provides a simple and direct way to determine reliability index if the probability of failure is known using numerical simulation.

The objective of this study is to determine post impact performance reliability of the connector embedded within the ABC pier struck by semi-trailer. The numerical simulation has been carried out by using finite element method (FEM). The results are then captured and utilized in this study to determine the DAF of the single coupler under axial compression and shear load. The DAF determined analytically is compared with the FE simulation results presenting a well agreement between the two providing valuable information and usefulness to aid in the selection of suitable connector utilized in ABC beyond those are presently deployed.

2. Methodology

In this study, connectors embedded in a prototypical pier foundation cap along with reinforcing steel bar is evaluated for their performance under high velocity semi-trailer impact loading. Post impact performance level comprising of material properties and composite behavior is determined by apportioning the load transferred to each coupler. The investigation is carried out through analytical methods by validating with FEA utilizing the material properties extracted from manufacturer's data. To examine the material behavior and failure pattern, FEA have been conducted for static and dynamic analyses. Experimental data was also extracted to evaluate the DAF. The FE models and respective simulations are carried out using the commercially available software package, ANSYS WORKBENCH. DAFs computed using FEA and from analytical methods are compared to validate the results via integrity analysis (IA).

DAFs of the reinforcing steel bar and coupler are determined from using material properties at short duration vehicle impact. The obtained DAFs are utilized to determine the reliability index of the embedded coupler at post impacted ABC pier. The performances are then evaluated by determining probability of failures (P_f) and corresponding performance reliability. IA has been conducted to validate results depicting stress and strain using conservative dynamic impact analyses captured from FEA [10]. The post impact performance results are utilized to determine reliability assessment through integrity analyses [12] by using the Hasofer-Lind reliability method [13] and relatively simplified approximation method for ABC [11,14] to avoid complexities and uncertainties. Efficacy of using ABC pier over the traditional cast-in-place RC bridge pier is shown by introducing performance function and reliability assessment via IA from conservative dynamic simulation results. This is further validated through comparing the performance

reliability as standardized for the half-sized and prototyped bridge pier component [7].

2.1. Materials and Geometric Properties

For this study, splice-sleeve dimensions as detailed by the manufacturer are shown in Figure 1[15, 16]. The embedded

main steel bar is placed inside the splice-sleeve, then grouted inside the coupler, and disconnected to provide the transference of load. Steel bars are disconnected in the middle of the grout using a 'Rebar Stop' as shown in Figure 1. The splice-sleeve connector used is made of cast-iron, and the manufacturer's data extracted and utilized to generate FEA.

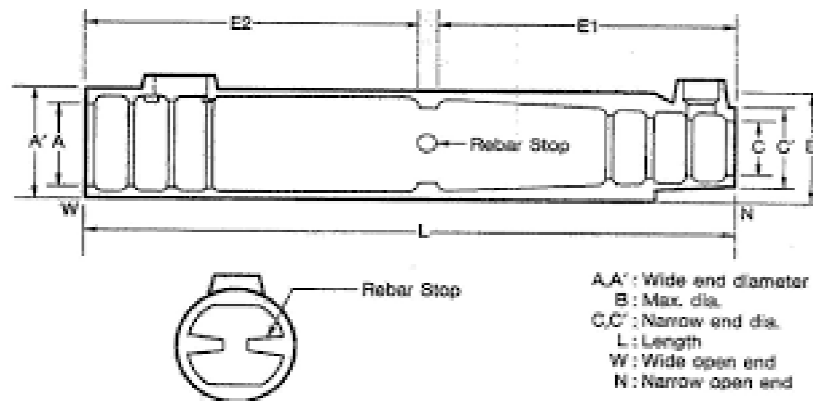


Figure 1. Splice-sleeve in Figure 1[15].

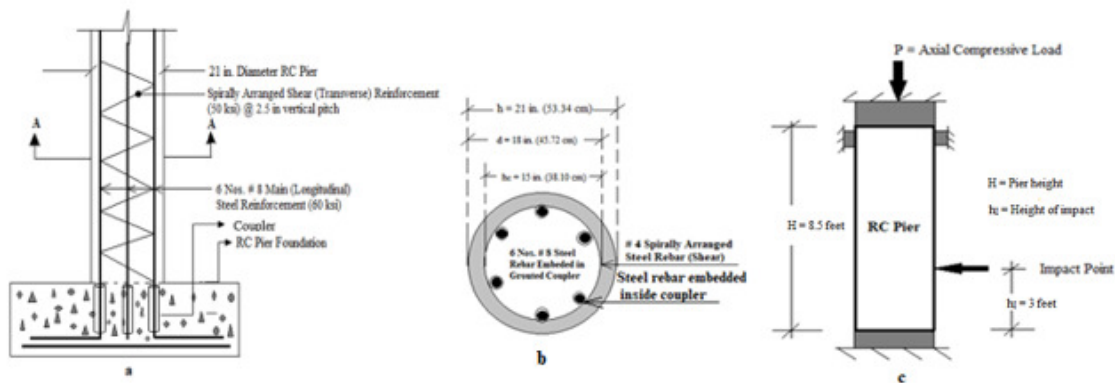


Figure 2. (a) Pier with Grouted coupler (b) Section A-A, and (c) End conditions of pier and impact point.

In this study, splice-sleeve number 8U-X connectors are utilized along with # 8 ASTM 706 bars used for the main or

longitudinal reinforcement. Geometrical details of the splice-sleeve [15] have been extracted, as shown in Table 1.

Table 1. Geometries of splice sleeve 8U-X [15].

Zone	Coupler Type	Internal Diameter (in.)(mm)	External Diameter (in.)(mm)
W = Wider End	8U-X	1.89(48.01)	2.52(64.01)
N = Narrower End	8U-X	1.3(33.02)	2.52(64.01)

The grouted couplers are strategically placed in a location where plastic hinges are highly expected to be occurred at the pier-foundation connection [17]. In this study, couplers are placed as shown in Figure 1(a). Grouted coupler embedded in pier is also shown in Figure 1 (b). Pier has been modeled with both ends restrained from rotation and deflection with unsupported length of 8.5 feet and the location of vehicle impact is considered at a distance 3 feet height from the foundation top, as shown in Figure 1(c).

2.2. Determination of Flexural Resistance

In this study, flexural performances of the connector embedded at pier foundation is studied at impact. Computations of axial loads on the pier and the partitioned load carried by each steel rebar are computed, with a semi-trailer considered as the vehicle weight for impact [18]. Computation of the axially compressive load incurred by the circular RC bridge pier, as shown in Figure 2 is carried out according to Equation 1 [19]. Axial compression load from the pier transmitted to individual reinforcing steel bar ($P_{n,s}$) has been approximately assessed by apportioning the load,

and using area ratio ($A_{coupler}/A_{net}$). The axial compression load that is directly transmitted into the respective coupler after impact through steel bar is as shown in Equation 2.

$$P_n = 0.85f'_c(A_g - A_{st}) + A_{st}f_y \quad (1)$$

$$P_{n,s} = P_n \left(\frac{A_c}{A_n} \right) \quad (2)$$

Where: P_n and $P_{n,s}$ indicate axial compression capacities of the RC pier and individual steel bar respectively; A_g , A_{st} , A_n , $A_{n,s}$ and A_c address gross cross-sectional (c/s) area of pier, area of total reinforcing steel bar provided in the pier section, net c/s area of the pier, c/s area of each steel reinforcing bar, and c/s area of hollow splice-sleeve respectively; f'_c and f_y designate the 28-day characteristic compressive strength of concrete and first yield stress of steel respectively.

The resulting values of axial compressive load experienced by the RC pier and partitioned load incurred by individual coupler conforming material and geometric properties using Equations 1 and 2 are shown in Tables 2 and 3 respectively.

Table 2. Pier geometries.

f'_c (ksi) (MPa)	f_y (ksi)(MPa)	A_g (in ²) (mm ²)	A_{st} (in ²) (cm ²)	A_n (in ²) (cm ²)	$A_{n,s}$ (in ²) (cm ²)	A_c (in ²) (cm ²)
3 (20.68)	60 (413.68)	346.50 (2235.48)	4.70 (30.32)	341.80 (2205.16)	0.780 (5.03)	2.20(14.2)

Table 3. Design loads.

P_n (kips) (kN)	$P_{n,d}$ (kips) (kN)	$P_{n,s}$ (kips) (kN)
1308.20 (5819.16)	1310 (5827.17)	3.01 (13.38)

2.3. Determination of Dynamic Amplification Factor (DAF)

The DAF is termed as the ratio of the dynamic to static strength of the structural element [20]. Reinforcing steel bar being an homogeneous and isotropic material, dissipates high energy and withstand substantial impact [21]. This leads very significant to determine DAF. In this study, vehicle weight (M) and impact velocity (V) of the semi-trailer are considered as 42.11 kips. (187.30 kN) and 100 ft/sec (30.48 m/sec) respectively [22]. The applied vehicular speed is taken from standardized permissible vehicular speeds [22, 23]. Determination of DAF due to vehicular impact and corresponding dynamic performance of reinforcing steel are studied at a quasi-static to high strain rate loading. The

dynamic flow stress (σ_d) as a first step to evaluate DAF in the reinforcing steel at impact is determined using Equation 3, as recommended by [2].

$$\sigma_{dyn} = \sigma_y \left[1 + \left(\frac{\dot{\epsilon}}{C} \right)^{1/p} \right] \quad (3)$$

Where: σ_y is the static flow stress for ASTM A706 Grade 60 steel bar [24] and is considered as 60 ksi (420 MPa); C addresses the material coefficient, and p is the strain rate parameter considered as 40 and 5 respectively [25]. The quasi-static strain rate of the steel reinforcing bar ($\dot{\epsilon}$) is considered as 0.16 s^{-1} for the vehicle velocity ranges at 100 ft/sec (30.48 m/s) [22].

Using the assumed values and Equation 3, σ_{dyn} is

calculated to be 79.80 ksi (550.20 MPa) [2].

The following step is to evaluate a constant, ξ [24] by utilizing Equation 3.

$$\xi = 0.019 - 0.009 * \left(\frac{\sigma_d}{60}\right) \quad (4)$$

Where: ξ is a dynamic parameter which depends on the dynamic yield stress of steel at the strain hardening zone ($\dot{\epsilon}$), and σ_{dyn} is the dynamic flow stress.

Equation 4 yields ξ as 0.0172

The DIF can be finally determined by using Equation 5 [26, 27]. Inserting the previous calculated values of $\dot{\epsilon}$ and ξ from the Equations 3 and 4 into Equation 5, DAF can be determined.

$$DAF = \left(\frac{\dot{\epsilon}}{10^{-4}}\right)^\xi \quad (5)$$

Equation 5 yields a DAF of 1.053.

2.4. Determination of Analytical Static and Dynamic Forces Due to Impact

The Static impact force on the pier (F_I) due to vehicular collision can be computed using Equation 6. In this study, the static moment (M_s) is computed at the top of the foundation which is also taken as the top of the coupler and multiplying F_I by the height of impact (h). The height of impact (h_I) is considered as 3 ft. (1 mtr.) from the pier base according to the specification for the frontal dimension of a semi-trailer [28].

$$F_I = \frac{wV}{\tau} \quad (6)$$

Where: F_I is the static impact force, W is the semi-trailer weight (considered as 42,108 lbs or 187.30 kN); V is the maximum permissible velocity taken as 100 ft/sec (30.48 m/sec) and the impact duration τ , is considered as 40 ms [29, 30]; Inserting these values into Equation 5, results F_I as 105,270 kip-ft/sec².

The corresponding static moment (M_s) experienced by the pier from the vehicle impact is determined by using Equation 7. h_I

$$M_s = F_I \cdot h_I \quad (7)$$

Where: F_I is the static impact force, and h_I is the impact point from the pier base.

Using the apportioned load after multiplying M_s by the area ratio (A_c/A_n), the static moment experienced by each coupler ($M_{s,c}$) can be approximately computed from Equation 8.

$$M_{s,c} = M_s \left(\frac{A_c}{A_n}\right) \quad (8)$$

The corresponding dynamic moment incurred by each coupler ($M_{d,c}$) is then computed from Equation 9 by multiplying $M_{s,c}$ with DIF.

$$M_{d,c} = DAF \cdot M_{s,c} \quad (9)$$

Where: $M_{s,c}$ and $M_{d,c}$ represent static and dynamic moments incurred by each coupler from vehicle impact due to load transmittance, and DAF has been explained in section 2.3.

Using the previously stated values substituted into Equation 8 yields $M_{s,c}$ of 22.26 kip-ft (30.17 kN-mtr) incurred by each coupler. The corresponding dynamic moment ($M_{d,c}$) computed from Equation 9, yields 23.44 kip-ft, (30.18 kN-mtr). As the dynamic properties cannot be estimated directly due to short duration collision, it can indirectly be thus evaluated from the analytical computation using the DIF of the reinforcing steel rebar [8].

2.5. Finite Element Analysis (FEA)

In this research, a numerical model developed using finite element analysis (FEA) is used to predict the individual coupler performance at post vehicle impact. FEA for static and dynamic behavior are developed using the commercial package ANSYS. For simplicity, a hollow cylindrical cast iron splice-sleeve (36 ksi or 248 MPa) is utilized along with 6 ksi (41.36 MPa) grout strength and # 8 steels rebar embedded into the grout (Figure 2). The cross-section utilized to generate meshing for the entire grouted coupler model is shown in Figure 3. Material properties utilized for developing numerical models are shown in Table 4. For all different material connections, non-separable contacts are utilized in the simulations. Reinforcing steel embedded inside the coupler and extended from coupler on both sides as shown in Figure 3. The external peripheral surface of the splice-sleeve is considered as fixed and non-separable. The embedded edge of rebar (6 in) is also considered as fixed as it is inserted and placed within the foundation concrete. The larger end (8 in) of the opposite side of the rebar is considered as free and is as shown in Figure 3 (a). FEM are generated in a conservative way where the apportioned axially compressive load is transmitted, and fractioned moment is applied to the free end of individual bar using area ratio (A_c/A_n). The apportioned load for axial compression ($P_{n,s}$) of 3.01 kips (13.4 kN) and static moment (M_s) of 22.26 kip-ft. (30.17 kN-m) applied on the free end are shown in Figure 3 (a). End conditions of the individual coupler-steel bar model along with the transmittance of compressive axial ($P_{n,s}$) load and horizontal impact load from vehicle collision experienced by the reinforcing steel are also shown in Figure 3. FEA of the single grouted coupler has been conducted using the apportioned load as stated in Section 2.4.

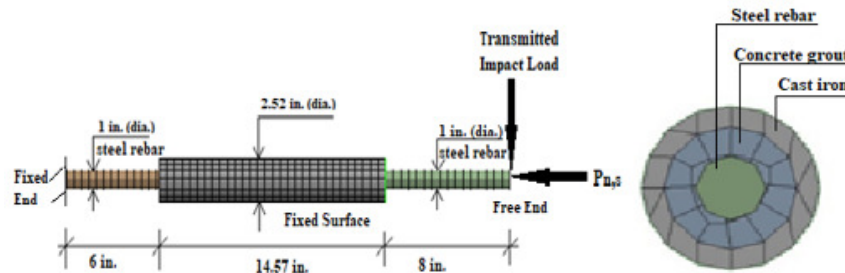


Figure 3. (a) End conditions of coupler-rebar model for FEM, and (b) Cross-section of FEA Model.

Table 4. Material properties.

SL. No.	Properties	Cast Iron	Grout	Steel Bar
1	Density (pci)	0.284	0.083	0.284
	(kN/m ³)	(77)	(22.53)	(77)
2	Young's Modulus (psi)	29*10 ⁶	43.51	29*10 ⁶
	(MPa)	(2*10 ⁵)	(0.3)	(2*10 ⁵)
3	Poisson's Ratio	0.3	0.3	0.3
4	Bulk Modulus (psi)	2.42*10 ⁷	2.26*10 ⁶	2.42*10 ⁷
	(MPa)	(1.6*10 ⁵)	(1.6*10 ⁴)	(1.6*10 ⁵)
5	Shear Modulus (psi)	1.12*10 ⁷	1.84*10 ⁶	1.12*10 ⁷
	(MPa)	(7.7*10 ⁴)	(1.26*10 ⁴)	(7.7*10 ⁴)
6	Tensile Yield Strength (psi)	3.62*10 ⁴	0	3.62*10 ⁴
	(MPa)	(249.6)	0	(249.6)
7	Tensile Ultimate Strength (psi)	3.62*10 ⁴	0	6.67*10 ⁴
	(MPa)	(249.6)	0	(459.8)
8	Compressive Ultimate Strength (psi)	0	5.95*10 ³	0
	(MPa)	0	(41.02)	0

2.6. Performance Reliability of Coupler in ABC Pier

The reliability of a structure is stated as its ability to meet the demands required of it over a defined period of time [13]. Reliability analysis is a process of determining the effect of variables on the performance of the design elements and system with a view to minimizing the probability of failure occurring. Structural systems and their constituent

components are designed to be load resisting systems. Complex structural systems have their reliability appraised from predictive models using probabilistic methods [31]. Exceedance of the capacity or resistance in the function by the load or demand component results in a failure and vice versa. Performance function (P) conforms a non-linear trend of strain, stress concentration and the corresponding dynamic material moduli using the regression analysis as shown in Figure 4.

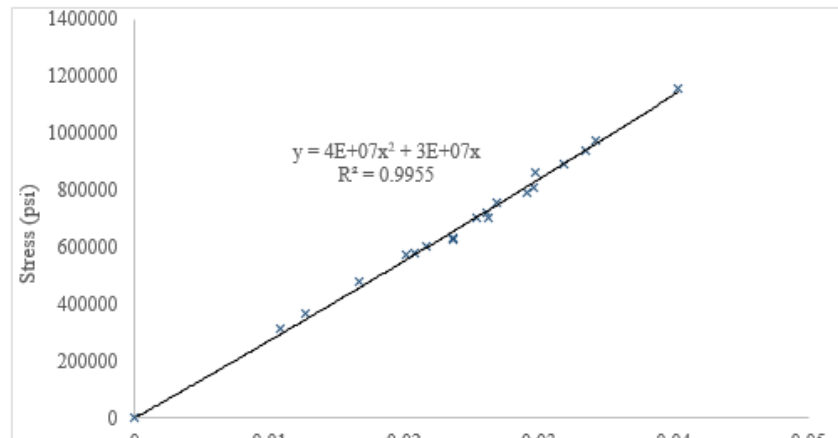


Figure 4. Dynamic Stress and Strain Relationship to capture material properties.

From Figure 4, Von Mises stress and corresponding strain plotted from dynamic simulations can capture the material property (dynamic modulus of elasticity) via regression analysis, come up with non-linear trend of performance function (P) of stress concentration and the corresponding strain with R^2 value is considered as 0.99. P is also considered to determine the post impact integrity criteria of coupler composite material is as shown in Equation 10.

$$P(\sigma, \varepsilon) = \sigma - 4.10^7 \cdot \varepsilon^2 - 3.10^7 \cdot \varepsilon(10)$$

Where: P , σ , and ε are already explained.

2.6.1. Integrity Analysis (IA) to Determine Reliability Index (β)

In order to mitigate discrepancies between static and dynamic simulations results, complexities involved to capture material modulus as a post impact performance, and exceedance of dynamic over static and material modulus, dynamic results for material modulus as demand are considered to ensure post impact criteria. The statistical data including mean (μ), covariance (V) and standard deviation (SD) of dynamic simulation results used to determine post impact performance reliability (β) are given in Table 4.

Table 5. μ , V and SD for stress (σ), strain (ε) and modulus of material (E).

Variables	μ	V	SD
σ (psi)	$6.74 \cdot 10^5$ (psi)	0.383	$2.58 \cdot 10^5$ (psi)
ε	0.024	0.38	0.0091
E (psi)	$2.65 \cdot 10^5$ (psi)	0.237	$6.28 \cdot 10^5$ (psi)

Monte Carlo simulations being expensive and requiring millions of simulations, moment-based methods such as the Hasofer-Lind [13] reliability index (β) method is one of these methods that was developed as an alternative to the simulations and has been recognized as an effective and precise method to estimate structural safety [6]. This method is considered in this study for its advantage over other moment-based methods including its invariance to the specific form of the P and not requiring prior knowledge of the distributions of the variables. The Hasofer-Lind reliability index is computed using an iterative procedure involving reduced variates, using factor of Safety (F) from

the materials integrity, capturing data from FEA and variables as computed in [13]. The reliability of index (β) is computed via integrity analyses using factor of safety (F) resulted from FEA given in Table 4 and is as shown in Equation 11 [32].

$$\beta = \frac{E \cdot (F) - 1}{SD \cdot (F)}(11)$$

Where: β is the reliability index, F (moduli of dynamic over static using numerical simulation) is the factor of safety computed from dynamic simulation results, E is the modulus of elasticity and SD is the standard deviation.

2.6.2. Direct Reliability Index

Performance reliability (β) of the individual coupler is further determined directly by using the probability of failures (P_f) resulted from dynamic simulation [11]. Results from the dynamic analysis is utilized as modulus of maximum elasticity (E) in demand utilizing dynamic DAF resulted from simulation (shown in Equation 10, E as 30×10^6 psi), as it exceeds the material E-modulus (29×10^6 psi). Maximum resulted stresses and strains from dynamic numerical simulations in terms of E-modulus in demand due to post impact behavior are captured to evaluate dynamic amplification effect (DAF) as 1.07 through the ratio of dynamic moduli (dynamic modulus / static modulus) draw an insightful correlation between DAF's computed analytically as 1.053. This result triggers to evaluate failures and corresponding reliabilities of coupler. Performance reliability (β) of the individual coupler can also be computed directly from probability of failure (P_f) is evaluated from the DAF's with a difference of 1.6 % which results as 0.0021 by using the inverse of the standard normal cumulative distribution functions of probability of failures (P_f) resulted from direct approximation method and is as shown in Equation 13 [13,33].

$$\beta = -\Phi^{-1}(P_f) \quad (12)$$

Where: P_f is the probability of failure and Φ^{-1} is the inverse of the standard normal cumulative distribution function.

2.6.3. Uncertainty Assessment using Confidence Interval (CI)

Confidence Interval (CI) has been utilized to capture the degree of uncertainty for assessing the FEA evaluated from dynamic simulation using normal distribution. CI can also determine the probability that a parameter ranges between a pair of values around the mean. Thus, CI is determined via using statistical parameters like mean (μ), standard deviation (SD), confidence level (z) and sample size (n) (Table 5) and is as shown in the Equation 13 [34].

$$CI = \mu \pm z \cdot \frac{SD}{\sqrt{n}} \quad (13)$$

Where: μ is the mean of sample size, SD is the standard deviation, n is the sample size, and z is the confidence or significance level considered as 95%.

3. Results and Discussions

Static analyses are conducted for the partitioned axial compression load, and the impact load experienced by a single grouted coupler/rebar connection. Further analyses using explicit dynamics are also undertaken, and the results including stress and strain are compared with the results incurred from static analysis. Substantial deformations are

observed from the results of both static and dynamic analyses, but failure is identified and determined to occur from the deformation at the junction of steel rebar undergoing dynamic analysis.

3.1. Results from FEM

3.1.1. Static Analysis

Results depicting maximum strain and stress from static analysis showing high strain concentrations and significant stresses are observed in the contact of grouted coupler and reinforcing steel rebar (as shown in Figures 5 and 6). Maximum permissible material modulus at dynamic impact (Maximum stress / Maximum strain) demand for the material performance evaluated from the simulation result subjected to static strain is 1.38 (Figure 4) and static stress (Figure 5) is 8.51×10^5 psi (5.8×10^3 MPa) which demands modulus of elasticity of the rebar at the coupler junction as 6.17×10^5 psi (7.57×10^5 MPa). This endorses material property is safe as E-modulus of reinforcing steel rebar is 29×10^6 psi. The integrity analyses from post impact performance comprising resulted stress and strain are performed to determine reliability analyses by utilizing the Hasofer-Lind reliability index (β) method [13].

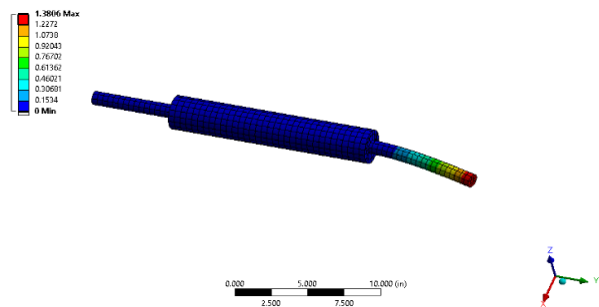


Figure 5. Static strain.

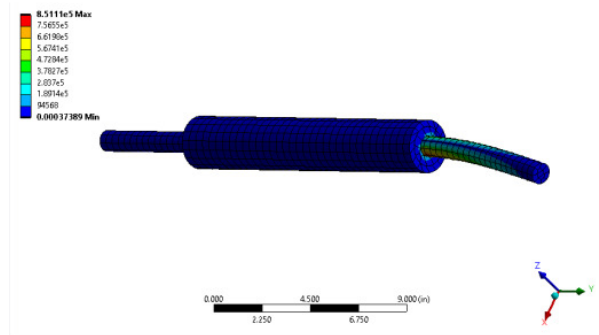


Figure 6. Static stress.

3.1.2. ExplicitDynamic Analysis

Explicit dynamic analysis shows significant deformation at steel bar, and maximum strain and stress concentrations resulted from at the contact of grout and reinforcing steel. Maximum permissible material modulus (considered as Maximum stress / Maximum strain) requirement is as shown in the simulation result subjected to respective dynamic strain and stress are 0.2 and 6.25×10^5 psi (1.82×10^5 MPa), showing the exceedance of E-modulus. The demand (dynamic) in material modulus from the study is computed as 31.25×10^6 psi (2.15×10^5 MPa) which minimally exceeds material E-modulus considered as 29×10^6 psi (2.1×10^5 MPa) by approximately 7.76%. However, integrity analysis [10] via demand of material moduli for dynamic over static using FEA (DAF) is computed as 1.07, whereas the analytical DAF has been computed as 1.053. This results a 1.6% difference in computing DAF. Highstrain showing deformation (Figure 7) and excessive stress concentration at reinforcing steel and coupler junction (Figure 8) control eventually the design parameters.

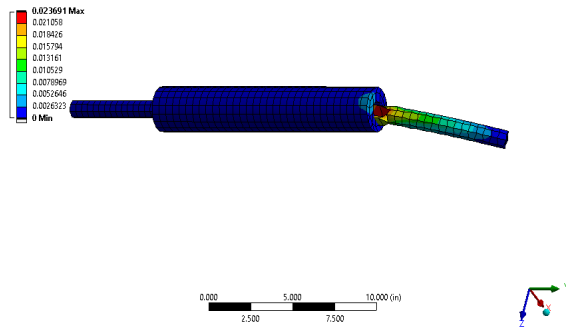


Figure 7. Dynamic Strain.

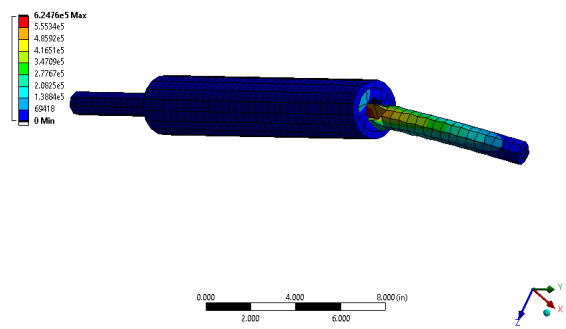


Figure 8. Dynamic Stress.

3.2. Performance Reliability of Coupler

The results comprising reliability indices based on vehicle impact performance for RC ABC pier is determined and as shown in Figure 9. This study has been carried out using FE model incorporating static and dynamic analyses.

Performance of coupler-embedded (ABC) RC pier is determined from the stress developed at coupler using the conservative results from dynamic simulation in experiencing high velocity vehicle impact.

3.2.1. Performance Reliability Using Integrity Analysis

Using Equation 11 and Table 4, β is evaluated from integrity analysis utilizing F results (F as 0.00516) yields 4.4 with a corresponding approximate P_f of 0.000005.

3.2.2. Performance Reliability Using Direct Reliability Method

Post impact performance as a reliability index (β) is also directly evaluated from probability of failure (P_f) as a function of DAF. Result from the dynamic analysis is utilized as dynamic modulus of material in demand using DAF resulted from simulation exceeding the material E-modulus. This result leads to evaluate failures and corresponding reliabilities of coupler. The performances are evaluated by determining probability of failures (P_f) and corresponding performance reliability through integrity analyses (IA) from resulting stress and strain from conservative dynamic impact. The IA of the impacted pier are conducted using resulted stresses and strains from FEA [10]. Stresses resulted due to impact and the dynamic amplification effect (DIF) draw an insightful correlation between DAF's computed analytically (1.053) and numerically using the FE simulation (1.07) through the ratio of moduli. Probability of failure (P_f) is evaluated from the DAF's with a difference of 1.6 % which results as 0.0021. Performance reliability (β) has been directly computed using Equation 13, yields as 2.86.

3.3.3. Determination of Reliability Index

Reliability Index (β) of the coupler can be determined using Sec. 3.2.1 and 3.2.2 from the corresponding probability of failures (P_f). The comparative results are put together and is as shown in Figure 9.

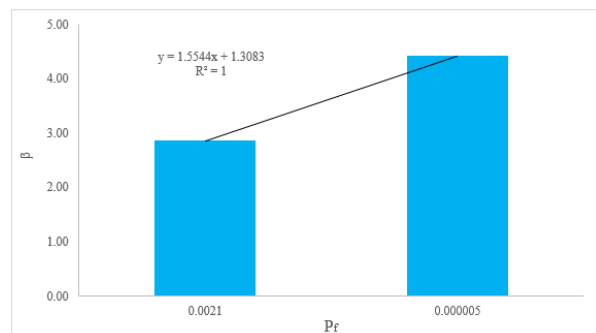


Figure 9. β from P_f

Using Figure 9, overall β of the coupler undergoing high velocity vehicle impact can be determined using the results of the regression analysis with R^2 value of 1 as shown in Equation 14.

$$\beta = 1.6.P_f + 1.31(14)$$

Where: P_f and β are already explained.

3.3.4. Uncertainty Assessment Using Confidence Interval (CI)

Confidence Interval (CI) has been utilized to measure the degree of uncertainty for assessing results evaluated from dynamic simulation comprising stress (σ), strain (ϵ), and post impact dynamic modulus (E) of the coupler material. The post impact dynamic results using CI for stress (σ), strain (ϵ), and modulus of coupler material (E) to capture the confidence level is shown in Table 5. The CI result depicting uncertainties in material properties portrays a substantial variation assessing post impact performance of coupler material. This warrants the manufacturing data which demands a decent increase to withstand specific dynamic load.

Table 5. Results of CI.

Variables	Confidence Value (CV)	Confidence Interval (CI)
σ (psi)	2.82×10^5	$(9.57 \times 10^5, 3.92 \times 10^5)$
ϵ	0.0041	(0.03, 0.02)
E (psi)	2.82×10^5	$(5.57 \times 10^5, -1.73 \times 10^4)$

4. Model Validation

To validate the model for strain variations along with the corresponding stress concentrations at the reinforcing steel rebar and coupler junctions, numerical (FE) simulation results are compared with the experimental data captured from the published journal [19]. The model shows a good agreement and positive coherence with the experimental results from published data [19] in terms of the stress - strain relationship, when apportioned load is transmitted to the single coupler. The result of the model validation is shown in Figure 10.

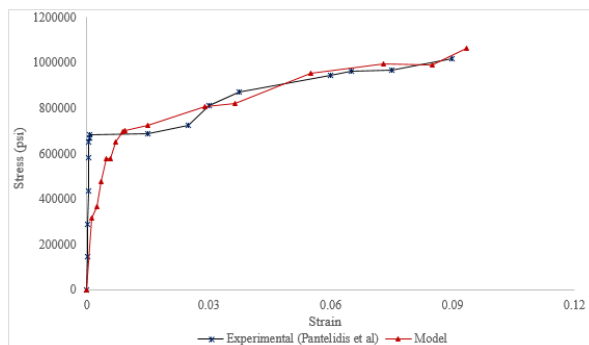


Figure 10. Model validation with experimental data [19].

5. Conclusions

In this research, an attempt is made to predict the post impact performance of splice-sleeve and grouted coupler for the flexural response at specific vehicle impact and position embedded at the pier – foundation. Reliability evaluation is carried out in this study to determine probability of failure and the corresponding post impact reliability of the coupler and compare the reliability performances via integrity results and direct reliability index. The following observations and conclusions are drawn from the study:

1. Numerical simulations (FEA) are used to determine performance reliability of coupler, and then compared and validated with the analytical results. DAF computed by using analytical methods and numerical simulations are quite similar, with a 1.6% difference. This indicates that current analytical methods used in computing the DAF are quite adequate for this purpose, comprising the model.
2. Reliability indices of the post impact performance of coupler material are determined from integrity analysis and direct reliability method. Direct reliability provides conservative reliability index compared to integrity analysis in order to capture non-linear performance of the coupler at specific vehicle impact performance of the coupler. CI analyses apprehend the uncertainties of using coupler materials extracted from manufacturer's data that warrants the material's property to withstand the specific dynamic load.
3. Overall coupler reliability evaluated from different method are utilized to determine β via using regression analysis provides a little conservative relationship. The Equation 14 can well apprehend to compute β if the P_f has been evaluated.
4. Furthermore, the model is compared with the experimental results extracted from published data as shown in Figure 10. This corroborates a good agreement between the trends of the results of stress-strain relationship using static simulation results.
5. This study instills an insightful knowledge and realistic correlation accomplishing usefulness of coupler embedded ABC pier-foundation. The efficacy of the coupler using in ABC system can be safely predicted by fulfilling the essential post impact performance criteria in addition to decreasing the construction time.
6. High precision experimental studies involving various geometries, material properties and different impact scenarios are recommended before considering coupler embedded ABC bridge piers at other positions for widespread use to withstand high velocity vehicle crash scenario.

Data Availability Some or all data, models, or code that support the findings of this study are available from the corresponding author upon reasonable request.

Acknowledgments

Funding to support this research was provided by the Mountain-Plains Consortium, a competitively selected University Transportation Center sponsored by the U.S. Department of Transportation through its Research and Innovative Technology Administration and by NMB Splice-Sleeve, North America. Any opinions, findings, and conclusions or recommendations expressed in this publication are those of the author(s) and do not necessarily reflect the views of NMB Splice-Sleeve, North America, or those of the U.S. Department of Transportation.

Abbreviations

f'_c	Concrete Strength
A_g	Gross c/s area of pier
A_{st}	Cross sectional area of reinforcing steel
A_{net}	Net cross-sectional area of pier
$A_{n,s}$	Cross-sectional area of each steel rebar
A_{CI}	Cross-sectional area of splice sleeve (cast iron)
A_{Grout}	Cross-sectional area of grout
$A_{coupler}$	Cross-sectional area of hollow splice-sleeve
E_{CI}	Material modulus of cast iron
E_{Grout}	Material modulus of grout, concrete
$E_{Concrete}$	Material modulus of concrete
E_{st}	Material modulus of reinforcing steel rebar
η	Energy dissipation
f_y	Yield strength of steel
P_n	Axial load of RC pier
$P_{n,s}$	Axial load of reinforcing steel rebar
$P_{n,s}$	Scaled-down design axial rebar load
σ_{dyn}	Dynamic flow stress
σ_v	Static flow stress
$\dot{\epsilon}$	Quasi-static strain rate of steel re-bar
h	Pier diameter
h_I	Height of impact from pier base
σ	Stress
ϵ	Strain
E	Modulus of elasticity of coupler
σ_D	Stress
ϵ_D	Strain
E_D	Modulus demand of coupler at dynamic impact
ξ	Dynamic parameter
C and p	Material Constants
I_S	Static impact force
W	Vehicle weight
M_s	Static moment for each coupler
$M_{s,c}$	Static moment incurred by each coupler
$M_{dyn,c}$	Dynamic moment incurred by each coupler
M_{dyn}	Dynamic moment for each coupler
t	Impact duration (sec)
DIF	Dynamic Increase Factor
CI	Confidence interval
μ	Mean
SD	Standard deviation,
Z	Confidence level
N	Sample size

Conflicts of Interest

The author declares no conflicts of interest.

References

- [1] Hauksson E, Kanamori H, Stock J, Cormier M-H, Legg M. Active Pacific North America Plate boundary tectonics as evidenced by seismicity in the oceanic lithosphere offshore Baja California, Mexico. *Geophys J Int Geophys J Int* 2014;196:1619–30. <https://doi.org/10.1093/gji/ggt467>
- [2] Feyerabend M. Hard transverse impacts on steel beams and reinforced concrete beams. Univ Karlsruhe (TH), Ger 1988.
- [3] Haber ZB, Saiidi MS, Sanders DH. Seismic performance of precast columns with mechanically spliced column-footing connections. *ACI Struct J* 2014;111:639–50.
- [4] Pantelides CP, Ameli MJ, Parks JE, Brown DN. Seismic evaluation of grouted splice sleeve connections for precast RC bridge piers in ABC. Utah Department of Transportation; 2014.
- [5] Sharma H, Gardoni P, Hurlebaus S. Performance-Based probabilistic capacity models and fragility estimates for RC columns subject to vehicle collision. *Comput Civ Infrastruct Eng* 2015;30:555–69. <https://doi.org/10.1111/mice.12135>
- [6] Nowak AS, Szerszen MM. Structural reliability as applied to highway bridges n.d.
- [7] Ghasemi SH, Nowak AS. Target reliability for bridges with consideration of ultimate limit state. *Eng Struct* 2017;152:226–37. <https://doi.org/10.1016/j.engstruct.2017.09.012>
- [8] Kowalsky MJ. Deformation limit states for circular reinforced concrete bridge columns. *J Struct Eng* 2000;126:869–78.
- [9] Roy S, Unobe ID, Sorensen AD. Investigation of the performance of grouted couplers in vehicle impacted reinforced concrete ABC bridge piers. *Adv Bridg Eng* 2022;3:1–30.
- [10] Alipour R, Farokhi Nejad A, Izman S. The reliability of finite element analysis results of the low impact test in predicting the energy absorption performance of thin-walled structures. *J Mech Sci Technol* 2015;29:2035–45. <https://doi.org/10.1007/S12206-015-0424-3>
- [11] Kharmanda G, El Hami A. Probability of Failure/Reliability Index. *Reliab Biomech* 2016:235–235. <https://doi.org/10.1002/9781119370840.APP4>
- [12] HASOFER AM. Reliability Index and Failure Probability. <http://DxDoiOrg/101080/03601217408907254> 2007;3:25–7. <https://doi.org/10.1080/03601217408907254>
- [13] Nowak AS, Collins KR. Reliability of structures. CRC Press; 2012.
- [14] Billinton R, Allan RN. Approximate system reliability evaluation. *Reliab Eval Eng Syst* 1983:282–301. https://doi.org/10.1007/978-1-4615-7728-7_11

- [15] ICC-ES Report. 2016. Explosive Blast Loads 2012.
- [16] ICC-ES Evaluation Report ESR-3433. 2014.
- [17] Ebrahimpour A, Earles BE, Maskey S, Tangarife M, Sorensen AD. Seismic performance of columns with grouted couplers in Idaho accelerated bridge construction applications. Idaho. Transportation Dept.; 2016.
- [18] AFDC. Vehicle Weight Classes & Categories. Altern Fuels Data Centre, US Dep Energy 2018.
- [19] Ameli MJ, Pantelides CP. Seismic analysis of precast concrete bridge columns connected with grouted splice sleeve connectors. *J Struct Eng* 2017;143:4016176.
- [20] Chopra AK. Dynamics of Structures, Theory and Applications to Earthquake Engineering. 2nd ed. Upper Saddle River: Pearson-Prentice Hall; 2001.
- [21] Roy S, Sorensen A. Energy Based Model of Vehicle Impacted Reinforced Bridge Piers Accounting for Concrete Contribution to Resilience. 18th Int. Probabilistic Work. IPW 2020, vol. 153, Springer Nature; 2021, p. 301.
- [22] Speed limits in the United States - Wikipedia n.d. https://en.wikipedia.org/wiki/Speed_limits_in_the_United_States (accessed April 24, 2020).
- [23] Actual Speeds on the Roads Compared to the Posted Limits. 2004.
- [24] ASTM. A706/A706M – 15 Standard Specification for Low-Alloy Steel Deformed and Plain Bars for Concrete. *Astm Int* 2015:1–6. https://doi.org/10.1520/A0706_A0706M-16
- [25] Sharma H, Hurlbauss S, Gardoni P. Performance-based response evaluation of reinforced concrete columns subject to vehicle impact. *Int J Impact Eng* 2012;43:52–62. <https://doi.org/10.1016/j.ijimpeng.2011.11.007>
- [26] Malvar LJ, Crawford JE. Dynamic increase factors for steel reinforcing bars [C]. 28th DDESB Semin. Orlando, USA, 1998.
- [27] Roy, S., Unobe, I., and Sorensen AD. Vehicle-Impact Damage of Reinforced Concrete Bridge Piers: A State-of-the-Art Review. *J Perform Constr Facil Am Soc Civ Eng* 2021, 35(5) 03121001 2021;35. [https://doi.org/10.1061/\(ASCE\)CF.1943-5509.0001613](https://doi.org/10.1061/(ASCE)CF.1943-5509.0001613)
- [28] Thomas RJ, Steel K, Sorensen AD. Reliability analysis of circular reinforced concrete columns subject to sequential vehicular impact and blast loading. *Eng Struct* 2018;168:838–51.
- [29] Cowper G, Symonds P. Strain hardening and strain-rate effects in the impact loading of cantilever beam. *Brown Univ Div Appl Math* 1957:1–46.
- [30] Buth CE, Brackin MS, Williams WF, Fry GT. Collision Loads on Bridge Piers: Phase 2. Report of Guidelines for Designing Bridge Piers and Abutments for Vehicle Collisions 2011:100.
- [31] Netherton MD. Probabilistic Modelling of Structural and Safety Hazard Risks for Monolithic Glazing Subject to